Journal of Materials Chemistry

Cite this: *J. Mater. Chem.*, 2012, **22**, 9374

www.rsc.org/materials

PAPER

Activation of gold decorated carbon nanotube hybrids for targeted gas adsorption and enhanced catalytic oxidation†

Ludovic Dumée,[*ab] Matthew R. Hill,[*a] Mikel Duke,[b] Leonora Velleman,[c] Kallista Sears,[a] Jürg Schütz,[a] Niall Finn[a] and Stephen Gray[b]

Received 8th December 2011, Accepted 7th March 2012
DOI: 10.1039/c2jm16458b

Free standing assemblies of carbon nanotubes (CNTs), known as bucky-paper (BP), have been functionalised through the *in situ* plating of gold nanoparticles within the interstitial spaces in the BP. The nanoparticles are extremely small and well distributed at short plating times, so much so that the specific surface area of the BP is actually increased by the gold incorporation. These well distributed nanoparticles exhibit high enthalpy hydrogen storage and selective carbon dioxide adsorption over other gases, in particular methane. In concert with the conductive BP substrate, it has been demonstrated that these materials can also act as high turnover heterogeneous catalysts.

A. Introduction

Highly selective gas adsorbing materials have attracted wide interest as carbon capture and fuel cells, and thus stand as promising solutions to achieve sustainable development. While the major breakthroughs achieved in the past decades followed routes targeting selective gas sieving *via* adsorption within nano-structured activated combinatorial materials,[1–10] processing large amounts of well organized materials such as metal nanoparticles (NPs),[11] metal–organic frameworks (MOFs) or zeolites remains a challenge.

Specific gas sensing and adsorption on metallic nano-particles (NPs) have been investigated due to their inherently high surface reactivity and thermo-mechanical stability over other materials. To date the highest H_2 storage capacity was reported in the case of metal hydrides[12] and noble metals (such as Pd, or Au). Although H_2 adsorption on gold surfaces was demonstrated to be weaker than on palladium (up to 900 times its volume of hydrogen[13]), gold catalytic activity was shown to be enhanced for gold NPs.[14,15] The presence of gold NPs on GaN nanowires[16] was found to change the sensing capacity of the bare nanowires. For instance, the intensity/voltage characteristics of these hybrid ~5 nm NP nanowires exposed to H_2, CH_4, CO_2 or CO were found to enhance by up to 4-fold when compared to that of air. The critical limitation of their development remains so far the processing and exposure of large surface areas of metallic NPs within highly porous matrices composed of a naturally high specific surface area material to optimize the surface to volume ratio. The adsorption[17–21] and catalytic[11,15,22–25] properties of gold are well documented following Haruta's work in the 90's[25] and sub-10 nm NPs were shown to be suitable adsorption sites due to their electronic d-bands becoming harder to saturate, creating semi-metallic structures more sensitive to selective gas adsorption.[14,26] The oxidation of CO by various sizes of gold NPs was found to be up to 100 times higher with sub-2 nm NPs when compared to sub-12 nm NPs, therefore highlighting the importance of exposed surface area on catalytic reactions.[26]

Amongst the number of substrates available for NP growth, CNTs offer both a very high specific surface area and the advantage of being chemically and thermally[27,28] stable over a large range of temperatures. Specific modifications of the CNT outer graphene walls[29–31] have been repeatedly used as sites for targeted functionalisation and precursors for NPs decoration.[32–34] The enhanced electrochemical and catalytic properties of these metal decorated CNT composites[33,35–37] make them promising candidates for storage[38,39] and sensing[33,34,40–42] of gas[43,44] or chemicals.[45–47] Our approach in this work involves the growth of gold NPs by electroless deposition onto hydroxyl-functionalized CNTs. Free-standing assemblies of CNTs, called bucky-papers (BPs), were used here as a growth support for their high specific surface area[32,42,48] in order to expose large quantities of activated gold NPs within a confined volume.

Here we describe a route to plate BPs with gold NPs in confined volumes by electroless deposition,[49] harnessing their highly porous (>90%)[50] and mechanically stable structure. This is to the best of our knowledge, the first time that a route to grow gold NPs on CNTs within the pores of BPs has been proposed. Furthermore this route enables control of the composite porosity and NP size distribution. With such control we then demonstrate their potential use as a gas storage media and catalyst.

[a]*CSIRO Materials Science and Engineering, Clayton, Victoria, 3168, Australia. E-mail: ludo.dumee@hotmail.com*
[b]*Institute for Sustainability and Innovation at Victoria University, Werribee, Victoria, 3030, Australia*
[c]*School of Chemical and Physical Sciences, Flinders University, Bedford Park, Adelaide, South Australia, 5042, Australia*
† Electronic supplementary information (ESI) available. See DOI: 10.1039/c2jm16458b

B. Experimental section

1. Gold plating procedure

Self-supporting BPs were processed from chemical vapour deposition grown multiwalled CNTs as described in a previous study.[51] In short, the functionalized CNTs were then suspended in propan-2-ol by 5 repeated cycles of freezing at −17 °C followed by bath sonication as per the method developed in ref. 50 The CNT suspension was then filtered on top of a porous poly (ether sulfone) membrane to form a self-supporting BP. BPs were exposed for 10 min to a flow of UV induced ozone in order to form hydroxyl groups at the surface of outer CNT walls.[52,53] These groups are needed to both facilitate wetting of the CNTs by the plating solutions and as anchors for the initial plating reactions.

The procedure of electroless gold deposition within porous materials has been described by Martin *et al.*[54] and was previously used to fabricate pure gold nanotubes[48] in a three step protocol. During the first step, referred to as sensitization, the BPs were immersed in a tin solution of 0.026 M $SnCl_2$ and 0.07 M trifluoroacetic acid in a solvent of 50 : 50 methanol : water for 45 min followed by thorough rinsing in methanol for 5 min. Then in the second step, referred to as activation, the membrane was immersed in a solution of 0.029 M ammoniacal $AgNO_3$ for 30 min in order to plate the activated sites with silver, before being rinsed sequentially in methanol and water to remove any unplated metals and remaining chemicals. In the third step, referred to as displacement deposition, the silver coated membrane was immersed in the gold plating solution consisting of 0.079 M $Na_3Au(SO_3)_2$, 0.127 M Na_2SO_3, 0.625 M formaldehyde and 0.025 M $NaHCO_3$. The temperature of this bath was ~1 to 4 °C with pH = 8. Plating time was varied from 1 h up to 30 h, to control the amount of gold deposited, as well as the NP shape and the sample porosity. During the plating process depicted in ref. 48 the gold cations were reduced on negatively charged sites on the CNTs and grew as particles of a few nanometres in dimension. All chemicals used in this work were of analytical grade.

2. BP properties analysis

The gold content in the structure was determined by thermogravimetric analysis (TGA) (Perkin Elmer, TGA 7) with tests performed at a rate of 10 °C min^{-1} and up to 900 °C. Porosity measurements were carried out on an Accu Pyc II 1340 gas displacement pycnometer from Micromeritics at 19 Psi with helium in a 1 cm^3 chamber while the BET specific surface area was obtained by N_2 adsorption at 77 K on a Micromeritics Tristar 3000 after degassing the samples for at least 12 hours. Focused Ion Beam (FIB) milling was performed to produce Scanning Electron Micrographs (SEMs) at 5 keV, 52° of tilt and 5 cm working distance. The gallium (Ga) milling was performed with an initial beam current of 7 nA followed by cleaning steps at 0.1 nA. Eventually, pore size distribution was determined by perm-porometry on a capillary flow porometer from Porous Materials Inc. in wet-up/dry-up mode. Galwick and N_2 were respectively used as the wetting liquid and to pressurize the BP pores up to 500 psi.

3. Gas adsorption

The adsorption of N_2, CH_4 and CO_2 was performed at room temperature while that of H_2 was obtained at both 77 K (liquid N_2 temperature) and 87 K (liquid Ar temperature) on selected samples that exhibited interesting adsorption behaviours using a Micromeritics ASAP 2420. The samples were degassed for 12 hours at 150 °C (Fig. 6 – ESI†).

4. Catalytic activity determination

BPs were exposed to pure analytical grade pentanal at 70 °C in oxygenated $CDCl_3$ for either 2 or 24 h. The composition of the solution before and after being exposed to the catalytic influence of the BPs was analysed using Nuclear Magnetic Resonance (NMR) on a Bruker 400 MHz spectrometer.

C. Results and discussion

1. Materials properties

As shown in Table 1, the porosity and specific surface area of the BPs were clearly modified after gold deposition. Porosity decreased steadily from 90% for the bare CNT BP down to 42% after 20 h of plating. Furthermore, pore size distribution was also highly modified with increasing plating time. A clear shift in pore size was visible towards smaller pores (Fig. 1) and tighter pore size distributions for increasing plating times. This is directly correlated to the amount of gold being deposited on the CNTs

Table 1 Properties of the gold–CNT hybrid composites—the particle size was estimated from the SEM images in Fig. 2

Samples, plating time (h)	Gold content, wt%	Porosity, (%)	Specific surface area, $m^2\ g^{-1}$	NP size range, nm
0	0	90	197	N/A
1	8	85	310	10–50
5	28	76	229	50–300
10	89	63	88	N/A
20	90	42	37	N/A

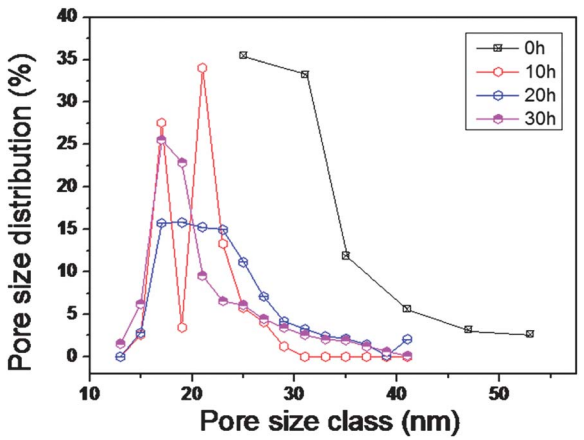

Fig. 1 Pore size distribution determined by porometry at various plating times.

and to the formation of nano-clusters bridging the CNTs. The inner structure of the BPs was revealed by Focused Ion Beam (FIB) milling of their surface and taking Scanning Electron Micrographs (SEMs) and is presented in Fig. 2 Gold NPs (10–50 nm) first formed on the CNT surface (Fig. 2—1 h) before evolving into nano-clusters (1 h to 5 h) and then spreading between 5 h and 20 h towards an interconnected network of continuous gold. After 20 h, the CNTs were uniformly coated and large nano-clusters emerged on the exposed gold surface.

TGA performed on the series of samples showed an initial, diminished thermal stability which was attributed to the ozone treatment inducing defects on the CNT walls. However, after 10 h of plating the stability, compared to a non-treated sample, was recovered and improved. The samples were all stable up to 400 °C. The gold content calculated from the residual mass at 900 °C increased from 8 wt% after 1 h of plating up to 90 wt% after 20 h (Table 1).

Furthermore, the material was found to be thermally stable with a mass loss of only 3–5% up to 300 °C while severe degradation (95–97%) started occurring above 300 °C (Fig. 3).

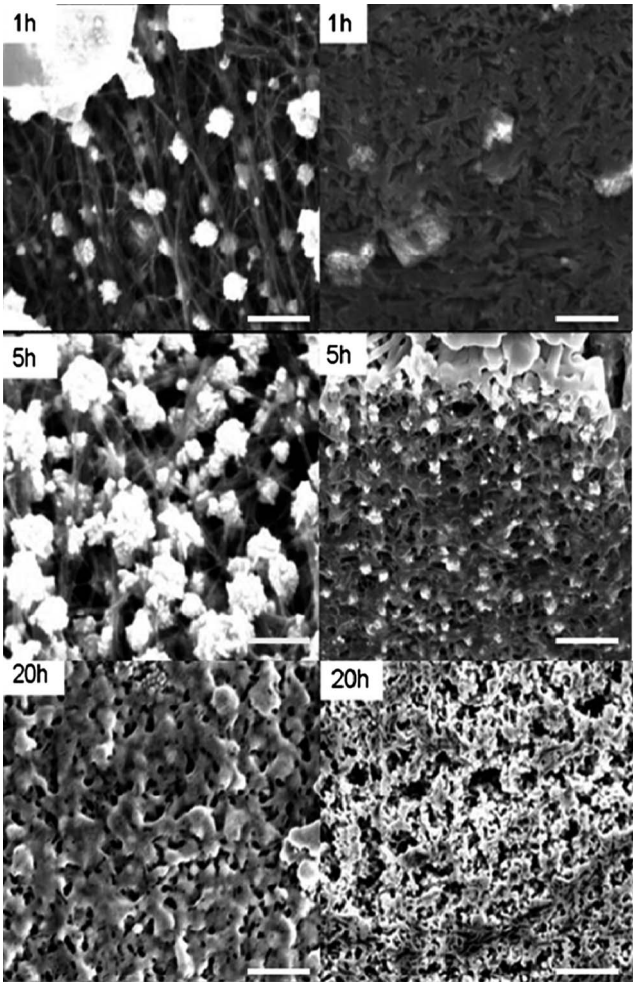

Fig. 2 SEMs of the surface (left column) and corresponding cross-sections (right column) taken at different plating times; the cross-sections were milled with a gallium beam from a Focus Ion Beam (FIB) column in the SEM; scale bars correspond to 500 nm on all the SEMs.

2. Gas adsorption

Gas adsorption was employed to investigate the distribution of Au NPs as a function of plating time. Nitrogen adsorption (Table 1) revealed that the specific surface area increases with plating times up to five hours, then subsequently decreases as plating continues. This indicates that the Au is initially deposited in nanoparticulate form, itself contributing to the surface area. Longer plating times increased the size of these particles, filling the voids and lowering the available surface area.

Successful exposure of the Au NPs on the BP surface was confirmed by measuring the enthalpy of adsorption towards hydrogen. Carbonaceous surfaces will typically adsorb hydrogen at around 4–5 kJ mol^{-1} (ref. 55) whereas metallated surfaces will form a stronger attraction to hydrogen, often between 5 and 50 kJ mol^{-1} depending on the metal alloy, surface roughness and crystallite morphology being tested.[56–58] Although the adsorption of extended gold surfaces has been demonstrated to be lower than that of other metals such as palladium or platinum,[59] recent work also demonstrated that small gold clusters lead to enhanced adsorption of hydrogen.[60,61] This is demonstrated in Fig. 2 and 4, where the average NP size was found to be around 52 and 300 nm (Table 1) for the 1 and 5 h plated samples, respectively. The

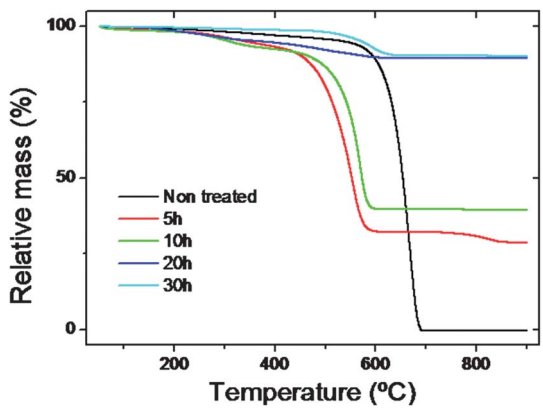

Fig. 3 TGA analysis results with plating time as the main parameter.

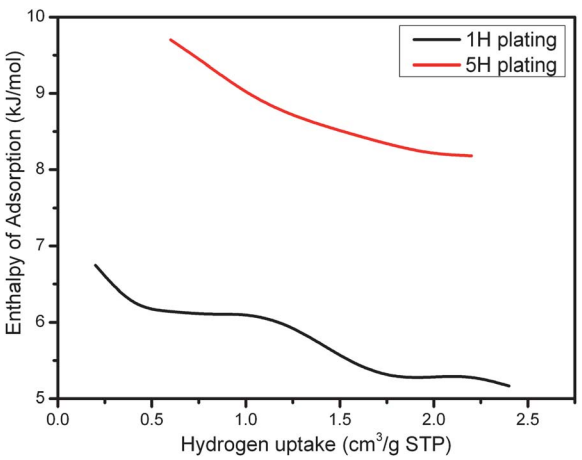

Fig. 4 The 5 h Au plated BP sample (top curve) showed higher enthalpy of adsorption for H_2 than the 1 h sample (bottom curve).

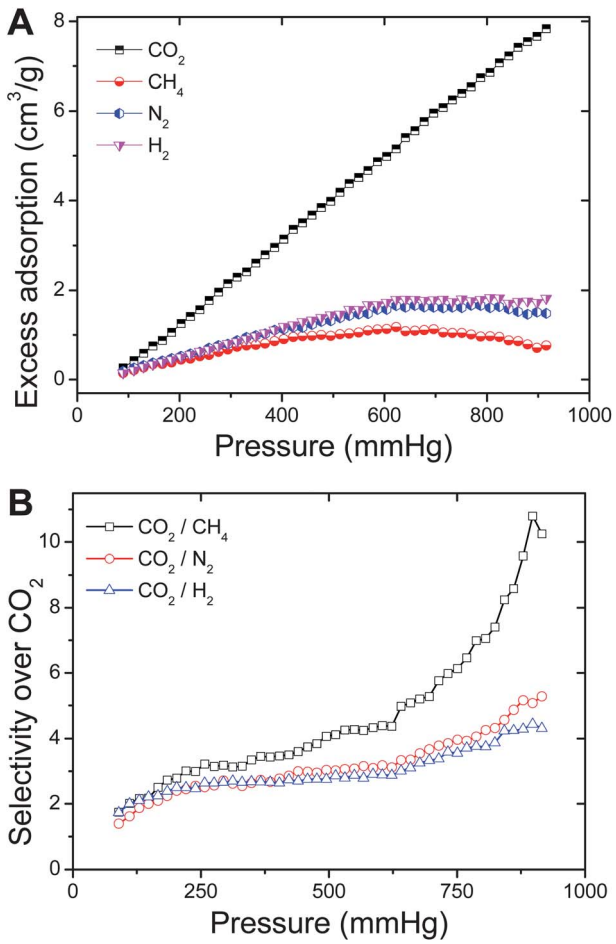

Fig. 5 Gas excess adsorption (A) and relative selectivity for CO_2 (B) over the other gases for the 5 h plated sample at room temperature.

Table 2 Catalytic decomposition of pentanal (%), when exposed to non-plated or gold plated CNTs for either 2 or 24 hours at 70 °C

	Pentanal after 2 h (%)	Pentanal after 24 h (%)
Control (no CNTs)	84.0	67.9
Non-plated BP	91.1	70.2
1 h Au plated BPs	64.3	36.7
10 h Au plated BPs	36.5	12.2

plating time is therefore clearly controlling NP morphologies and sizes, thus influencing the overall adsorption process. The largest hydrogen physisorption is found to occur for the 5 h plated sample giving a binding enthalpy as high as 9.8 kJ mol^{-1}. The clustering of the gold NPs is found, after 5 h of plating, to lead to a semi-continuous network covering the surface of the CNTs and starting to fill the pores. It is therefore likely that shorter plating times would lead to smaller NP size distributions that could possibly even possess higher hydrogen adsorption capacity.

Exposed Au NPs also deliver selective gas adsorption, as shown in Fig. 5. In particular, CO_2/CH_4 adsorption selectivity is as high as 11 at 900 mmHg. This is an important gas pair for industrial separations which could also lead to breakthrough towards more efficient and sensitive gas sensing materials.

3. Catalytic activity: pentanal decomposition

Gold is well known to play a part in catalytic oxidations.[11,15,22–25] Cost and recovery of the gold dictate that highly exposed surfaces that lower the amount of catalyst needed, or increase the reaction rates, are desirable. A heterogeneous catalyst where the active material is affixed to a support is also desirable as it avoids complicated recovery processes. To demonstrate the effects of the well-dispersed gold upon the conductive carbon substrate, oxidation of pentanal to pentanoic acid was explored (Table 2). Oxygenated solutions of pentanal were exposed to functionalised and non-functionalised BP (normalised to carbon content) at 70 °C for 2 and 24 hours. Table 2 shows that the oxidation is significantly enhanced by the gold functionalised BP, whilst non-functionalised samples showed no significant change from the control sample.

D. Conclusions

A novel route to well-distributed gold NPs on a BP substrate has been shown for the first time. The well-distributed gold NPs were observed only after a short plating time, and led to increased surface area. High enthalpy hydrogen adsorption demonstrated well-exposed gold surfaces, which showed selective gas adsorption, useful in particular for CO_2/CH_4 separations. The combination with the conductive BP substrate proved to be effective for developing a high turnover rate heterogeneous catalyst. These materials offer new applications in separations and chemical conversions.

Notes and references

1 H. Bux, C. Chmelik, J. M. van Baten, R. Krishna and J. Caro, *Adv. Mater.*, 2010, **22**, 4741–4743.
2 S. T. Meek, J. A. Greathouse and M. D. Allendorf, *Adv. Mater.*, 2011, **23**, 249–267.
3 E. Poirier and A. Dailly, *Nanotechnology*, 2009, **20**, 204006.
4 C. Zlotea, R. Campesi, F. Cuevas, E. Leroy, P. Dibandjo, C. Volkringer, T. Loiseau, G. Férey and M. Latroche, *J. Am. Chem. Soc.*, 2010, **132**, 2991–2997.
5 J. Ahn, W.-J. Chung, I. Pinnau and M. D. Guiver, *J. Membr. Sci.*, 2008, **314**, 123–133.
6 E. R. Hensema, *Adv. Mater.*, 1994, **6**, 269–279.
7 K. Sumida, M. R. Hill, S. Horike, A. Dailly and J. R. Long, *J. Am. Chem. Soc.*, 2009, **131**, 15120–15121.
8 M. C. Duke, J. C. D. da Costa, D. D. Do, P. G. Gray and G. Q. Lu, *Adv. Funct. Mater.*, 2006, **16**, 1215–1220.
9 M. C. Duke, J. C. Diniz da Costa, G. Q. Lu, M. Petch and P. Gray, *J. Membr. Sci.*, 2004, **241**, 325–333.
10 A. Tavolaro and E. Drioli, *Adv. Mater.*, 1999, **11**, 975–996.
11 H. Sakurai, S. Tsubota and M. Haruta, *Appl. Catal., A*, 1993, **102**, 125–136.
12 W. P. Kalisvaart, C. T. Harrower, J. Haagsma, B. Zahiri, E. J. Luber, C. Ophus, E. Poirier, H. Fritzsche and D. Mitlin, *Int. J. Hydrogen Energy*, 2010, **35**, 2091–2103.
13 W. Grochala and P. P. Edwards, *ChemInform*, 2004, **35**, 1283.
14 G. Bond, *Gold Bull.*, 2010, **43**, 88–93.
15 H. Sakurai and M. Haruta, *Appl. Catal., A*, 1995, **127**, 93–105.
16 C. A. Berven, V. Dobrokhotov, D. N. McIlroy, S. Chava, R. Abdelrahaman, A. Heieren, J. Dick and W. Barredo, *IEEE Sens. J.*, 2008, **8**, 930–935.
17 L. Stobinski and R. Dus, *Surf. Sci.*, 1992, **269–270**, 383–388.
18 L. Stobinski, R. Nowakowski and R. Dus, *Vacuum*, 1997, **48**, 203–207.
19 V. M. Browne, A. F. Carley, R. G. Copperthwaite, P. R. Davies, E. M. Moser and M. W. Roberts, *Appl. Surf. Sci.*, 1991, **47**, 375–379.

20 N. Lopez, T. V. W. Janssens, B. S. Clausen, Y. Xu, M. Mavrikakis, T. Bligaard and J. K. Nørskov, *J. Catal.*, 2004, **223**, 232–235.
21 S. Tibus, J. Klier and P. Leiderer, *J. Low Temp. Phys.*, 2006, **142**, 83–89.
22 S. Wang, Y. Zhao, J. Huang, Y. Wang, S. Wu, S. Zhang and W. Huang, *Solid-State Electron.*, 2006, **50**, 1728–1731.
23 G. Musie, M. Wei, B. Subramaniam and D. H. Busch, *Coord. Chem. Rev.*, 2001, **219–221**, 789–820.
24 K.-C. Wu, Y.-L. Tung, Y.-L. Chen and Y.-W. Chen, *Appl. Catal., B*, 2004, **53**, 111–116.
25 M. Haruta, *Catal. Today*, 1997, **36**, 153–166.
26 S. H. Overbury, V. Schwartz, D. R. Mullins, W. Yan and S. Dai, *J. Catal.*, 2006, **241**, 56–65.
27 A. E. Aliev, C. Guthy, M. Zhang, S. Fang, A. A. Zakhidov, J. E. Fischer and R. H. Baughman, *Carbon*, 2007, **45**, 2880–2888.
28 J. Che, T. Cagin and W. A. G. Iii, *Nanotechnology*, 2000, **11**, 65–69.
29 T. Lin, V. Bajapi, T. Ji and L. Dai, *Aust. J. Chem.*, 2003, **56**, 635–651.
30 M. Majumder, N. Chopra and B. J. Hinds, *J. Am. Chem. Soc.*, 2005, **127**, 9062–9070.
31 J. Zhao, D. W. Schaefer, D. Shi, J. Lian, J. Brown, G. Beaucage, L. Wang and R. C. Ewing, *J. Phys. Chem. B*, 2005, **109**, 23351–23357.
32 C.-Y. Chen, K.-Y. Lin, W.-T. Tsai, J.-K. Chang and C.-M. Tseng, *Int. J. Hydrogen Energy*, 2010, **35**, 5490–5497.
33 K.-Y. Lin, W.-T. Tsai and T.-J. Yang, *J. Power Sources*, 2010, DOI: 10.1016/j.powsour.2010.04.026.
34 Y. Yun, Z. Dong, V. N. Shanov, A. Doepke, W. R. Heineman, H. B. Halsall, A. Bhattacharya, D. K. Y. Wong and M. J. Schulz, *Sens. Actuators, B*, 2008, **133**, 208–212.
35 X. Chen, Y. Zhang, X. P. Gao, G. L. Pan, X. Y. Jiang, J. Q. Qu, F. Wu, J. Yan and D. Y. Song, *Int. J. Hydrogen Energy*, 2004, **29**, 743–748.
36 F. Tan, X. Fan, G. Zhang and F. Zhang, *Mater. Lett.*, 2007, **61**, 1805–1808.
37 J. John, E. Gravel, A. Hagege, H. Y. Li, T. Gacoin and E. Doris, *Angew. Chem., Int. Ed.*, 2011, **50**, 7533–7536.
38 J. J. Zhao, A. Buldum, J. Han and J. P. Lu, *Nanotechnology*, 2002, **13**, 195–200.
39 S. M. Cooper, H. F. Chuang, M. Cinke, B. A. Cruden and M. Meyyappan, *Nano Lett.*, 2003, **3**, 189–192.
40 D. R. Kauffman, Y. Tang, P. D. Kichambare, J. F. Jackovitz and A. Star, *Energy Fuels*, 2010, **24**, 1877–1881.
41 M. Kaempgen, M. Lebert, N. Nicoloso and S. Roth, *Appl. Phys. Lett.*, 2008, **92**, 3.
42 D. Yuan and Y. Liu, *Rare Met.*, 2006, **25**, 237–240.
43 H. Cong, J. Zhang, M. Radosz and Y. Shen, *J. Membr. Sci.*, 2007, **294**, 178–185.
44 R. Smajda, A. Kukovecz, Z. Konya and I. Kiricsi, *Carbon*, 2007, **45**, 1176–1184.
45 N. A. Kaskhedikar and J. Maier, *Lithium Storage in Carbon Nanostructures*, WILEY-VCH Verlag, 2009, pp. 2664–2680.
46 C. Liu, F. Li, L.-P. Ma and H.-M. Cheng, *Advanced Materials for Energy Storage*, WILEY-VCH Verlag, 2010, pp. E28–E62.
47 S. H. Ng, J. Wang, Z. P. Guo, J. Chen, G. X. Wang and H. K. Liu, *Electrochim. Acta*, 2005, **51**, 23–28.
48 L. Velleman, J. G. Shapter and D. Losic, *J. Membr. Sci.*, 2009, **328**, 121–126.
49 L. Dumee, L. Velleman, K. Sears, M. Hill, J. Schutz, N. Finn, M. Duke and S. Gray, *Membranes*, 2010, **1**, 25–36.
50 L. F. Dumée, K. Sears, J. Schütz, N. Finn, C. Huynh, S. Hawkins, M. Duke and S. Gray, *J. Membr. Sci.*, 2010, **351**, 36–43.
51 S. C. Hawkins, J. M. Poole and C. P. Huynh, *J. Phys. Chem. C*, 2009, **113**, 12976–12982.
52 S. Agrawal, M. S. Raghuveer, H. Li and G. Ramanath, *Appl. Phys. Lett.*, 2007, **90**, 193103–193104.
53 M.-L. Sham and J.-K. Kim, *Carbon*, 2006, **44**, 768–777.
54 V. P. Menon and C. R. Martin, *Anal. Chem.*, 1995, **67**, 1920–1928.
55 T. Ben, H. Ren, S. Ma, D. Cao, J. Lan, X. Jing, W. Wang, J. Xu, F. Deng, J. M. Simmons, S. Qiu and G. Zhu, *Angew. Chem., Int. Ed.*, 2009, **48**, 9457–9460.
56 C. Kartusch and J. A. van Bokhoven, *Gold Bull.*, 2009, **42**, 9457.
57 E. Bus and J. A. van Bokhoven, *Phys. Chem. Chem. Phys.*, 2007, **9**, 2894–2902.
58 S. J. Holden and D. R. Rossington, *J. Phys. Chem.*, 1964, **68**, 1061–1067.
59 S. A. C. Carabineiro and B. E. Nieuwenhuys, *Gold Bull.*, 2007, **42**.
60 L. Barrio, P. Liu, J. A. Rodriguez, J. M. Campos-Martin and J. L. G. Fierro, *J. Chem. Phys.*, 2006, **125**, 164715.
61 N. S. Phala, G. Klatt and E. v. Steen, *Chem. Phys. Lett.*, 2004, **395**, 33–37.

